Progress in Biophysics and Molecular Biology 98 (2008) 52–60

Contents lists available at ScienceDirect

Progress in Biophysics and Molecular Biology

journal homepage: www.elsevier.com/locate/pbiomolbio

Review

In silico risk assessment for drug-induction of cardiac arrhythmia

Shingo Suzuki [a], Shingo Murakami [a,b], Kenji Tsujimae [a], Ian Findlay [c], Yoshihisa Kurachi [a,b,*]

[a] *Division of Molecular and Cellular Pharmacology, Department of Pharmacology, Graduate School of Medicine, Osaka University, 2-2 Yamada-oka, Suita, Osaka 565-0871, Japan*
[b] *The Center for Advanced Medical Engineering and Informatics, Osaka University, 2-2 Yamada-oka, Suita, Osaka 565-0871, Japan*
[c] *CNRS UMR 6542, Faculté des Sciences, Université François-Rabelais de Tours, France*

ARTICLE INFO

Article history:
Available online 29 May 2008

Keywords:
Cardiac action potential
I_{Kr} blocker
Mapping
Cardiac arrhythmia

ABSTRACT

The main components of repolarization reserve for the ventricular action potential (AP) are the rapid (I_{Kr}) and slow (I_{Ks}) delayed outward K^+ currents. While many drugs block I_{Kr} and cause life-threatening arrhythmias including *torsades de pointes*, the frequency of arrhythmias varies between different I_{Kr}-blockers. Different types of block of I_{Kr} cause distinct phenotypes of prolongation of action potential duration (APD), increase in transmural dispersion of repolarization (TDR) and, accordingly, occurrence of *torsades de pointes*. Therefore the assessment of a drug's proarrhythmic risk requires a method that provides quantitative and comprehensive comparison of the effects of different forms of I_{Kr}-blockade upon APDs and TDR. However, most currently available methods are not adapted to such an extensive comparison. Here, we introduce I_{Kr}–I_{Ks} two-dimensional maps of APD and TDR as a novel risk-assessment method. Taking the kinetics of I_{Kr}-blockade into account, APDs can be calculated upon a ventricular AP model which systematically alters the magnitudes of I_{Kr} and I_{Ks}. The calculated APDs are then plotted on a map where the *x* axis represents the conductance of I_{Kr} while the *y* axis represents that of I_{Ks}. TDR is simulated with models corresponding to APs in epicardial, midcardial and endocardial myocardium. These two-dimensional maps of APD and TDR successfully account for differences in the risk resulting from three distinct types of I_{Kr}-blockade which correspond to the effects of dofetilide, quinidine and vesnarinone. This method may be of use to assess the arrhythmogenic risk of various I_{Kr}-blockers.

Contents

* Corresponding author. Division of Molecular and Cellular Pharmacology, Department of Pharmacology, Graduate School of Medicine, Osaka University, 2-2 Yamada-oka, Suita, Osaka 565-0871, Japan. Tel: +81 6 6879 3512; fax: +81 6 6879 3519.
E-mail address: ykurachi@pharma2.med.osaka-u.ac.jp (Y. Kurachi).

0079-6107/$ – see front matter © 2008 Elsevier Ltd. All rights reserved.
doi:10.1016/j.pbiomolbio.2008.05.003

1. Introduction

A number of drugs in clinical use and during development have had to be withdrawn because of their proarrhythmic side effects. These otherwise promising compounds are a risk for patients and force the pharmaceutical industry to bear enormous costs. *Torsades de pointes* is a malignant polymorphic ventricular tachyarrhythmia which is particularly associated with drug therapy and drugs with this adverse effect have been either withdrawn or labeled with strict use restrictions (Roden, 2004).

The delayed rectifier K^+ current, I_K, contributes to phase-2 and phase-3 repolarization of the cardiac ventricular action potential (AP) and influences action potential duration (APD). The rapidly activating K^+ current (I_{Kr}) and the slowly activating K^+ current (I_{Ks}) are two distinct components of I_K in many mammals including man (Sanguinetti and Jurkiewicz, 1990; Sanguinetti and Jurkiewicz, 1991; Wang et al., 1997). Many cardiac and non-cardiac drugs that cause life-threatening cardiac arrhythmias including *torsades de pointes* block I_{Kr}. Blockade of I_{Kr} prolongs cardiac APD and QT interval. The pore subunit of I_{Kr} is encoded by HERG (human *ether-a-go-go*-related gene) and several types of congenital long QT syndrome, which is often associated with *torsades de pointes*, are caused by loss of function mutants of HERG. Therefore, the compounds causing I_{Kr}-blockade were considered to have torsadogenic risk by prolonging QT interval.

Although the precise mechanism for drug-induction of cardiac arrhythmias is not yet understood, it is widely accepted that prominent prolongation of APD and QT interval due to I_{Kr}-blockade, especially in bradycardia, forms the substrate for the phenomena. However, an increasing mass of evidence shows that the occurrence of cardiac arrhythmias varies greatly between different I_{Kr}-blockers. The I_{Kr}-blockade potential of drugs, which is usually measured by testing their effects against the HERG channel expressed in either mammalian cells or *Xenopus* oocytes, and the drug-induced prolongation of APD and QT interval in animals are now not considered to be as closely associated with the torsadogenic risk as before (Belardinelli et al., 2003; Shah and Hondeghem, 2005; Lawrence et al., 2005; Hoffmann and Warner, 2006; Kannankeril and Roden, 2007; Hondeghem, 2006, 2007).

In addition to the prolongation of APD a number of other indicators of risk for *torsades de pointes* have been proposed. These include worsening of transmural dispersion of repolarization (TDR), triangulation of the cardiac AP, early afterdepolarization (EAD), and reverse frequency dependence effects of drugs. Accordingly, the methods of *in silico* prediction for drug-induced cardiac arrhythmias using cardiac AP models need to be reconsidered. Here we briefly review current understanding of the mechanisms for proarrhythmic action of drugs and the existing risk-assessment methods, and then introduce a new *in silico* method which has been developed in our laboratory for quantitative and comprehensive prediction.

2. Experimental risk assessments for drug-induced *torsades de pointes*

2.1. Relationship between APD prolongation and drug-induced torsades de pointes

For assessment of potential risk of drug-induced cardiac arrhythmia, the effects of a drug on the HERG channel expressed in either mammalian cells or *Xenopus* oocytes, and the prolongation of APD and QT interval in animals is now routinely measured. However, there are enough examples to indicate that these tests are not accurate or sufficient to assess the torsadogenic risk of drugs (Belardinelli et al., 2003; Shah and Hondeghem, 2005; Lawrence et al., 2005; Hoffmann and Warner, 2006; Hondeghem, 2006, 2007; Kannankeril and Roden, 2007). (1) Drug-effect prediction using expressed HERG channels can be inadequate in some cases. For example, the HERG channel current can be strongly blocked by clozapine which has no effect on frequency corrected QT interval (QTc) and lacks torsadogenic potential in human (Hoffmann and Warner, 2006; Warner and Hoffmann, 2002). Granisetron, ondansetron and dolasetron also block HERG channel current, but no cases of *torsades de pointes* associated with their use have been reported (Shah and Hondeghem, 2005; Kuryshev et al., 2000). (2) The blockade of I_{Kr} in ventricular tissue may not always be associated with torsadogenic risk. Tamoxifen potently blocks I_{Kr} in the ventricle but does not cause *torsades de pointes* (Liu et al., 1998). (3) Drug-induced prolongation of QT interval is not always associated with *torsades de pointes*. For example, ziprasidone prolongs QTc to a great extent but it has not been associated with *torsades de pointes* (Taylor, 2003). The reverse association is also not always true. Drugs that have been associated with *torsades de pointes* do not necessarily significantly prolong QT interval (Shah and Hondeghem, 2005; Morganroth, 1993). Sotalol can induce arrhythmia before any prolongation of the AP (Shah and Hondeghem, 2005; Hondeghem, 2000; Hondeghem and Hoffmann, 2003). On the contrary, prolongation of the QT interval can be antiarrhythmic in some cases as shown by the antiarrhythmic effects of amiodarone (Van Opstal et al., 2001). Therefore, it is possible that false screening has been conducted, based on the questionable association between I_{Kr}-blockade and proarrhythmic side effects.

2.2. Emerging predictors of drug-induced torsades de pointes

In addition to prominent prolongation of APD, it is now recognized that transmural dispersion of ventricular repolarization (TDR) and other properties, such as early afterdepolarization (EAD), reverse frequency dependence, and triangulation of the AP are associated with *torsades de pointes* (Belardinelli et al., 2003; Shah and Hondeghem, 2005).

Prolonged APD forms the substrate for increases in TDR and EAD, and not directly for *torsades de pointes*. An increase in TDR leads to heterogeneity of refractoriness in the ventricular tissue, which may serve as a substrate for re-entry which is an underlying mechanism for the perpetuation of *torsades de pointes*. EAD leads to ectopic beats which may be a trigger for re-entry, but TDR may be increased by EAD. Triangulation of the AP and prolonged APD in a reverse frequency-dependent manner are now recognized to be proarrhythmic because EADs can be easily evoked in these conditions. Therefore, phenotypes of a drug effects more complex than APD prolongation may determine the occurrence of life-threatening arrhythmia.

2.2.1. Transmural dispersion of repolarization

A drug-induced prominent prolongation of APD and an increase in TDR may be related or independent components of the substrate for re-entrant ventricular tachycardia, and an increase in TDR is associated with drug-induced *torsades de pointes* (Belardinelli et al., 2003). For example, sotalol prolongs APD more prominently in M cells than in epicardial or endocardial cells and thus may worsen TDR, leading to *torsades de pointes* (Yan and Antzelevitch, 1998). A good example illustrating the complex relationship between prolongation of APD, TDR and drug-induced *torsades de pointes* is the comparison of the effects of dofetilide and amiodarone: dofetilide prolongs APD during bradycardia and worsens TDR, while amiodarone causes prominent prolongation of APD but does not worsen TDR. This difference may explain why amiodarone rarely causes *torsades de pointes* while dofetilide often does so. Similar associations between TDR rather than APD prolongation and *torsades de pointes* can be found in many other drugs (Belardinelli et al.,

2003). Therefore, TDR should be considered as a predictor for drug-induced *torsades de pointes*, independently of APD prolongation.

2.2.2. Triangulation and early afterdepolarization

Triangulation of the AP is usually defined as prolongation of APD_{30-90} and as the name suggests this replaces the notch-and-dome morphology of the AP with an almost linear phase of repolarization (Shah and Hondeghem, 2005). Triangulation is reported to be a strong proarrhythmic predictor and may appear in the ECG as widened, flattened, or notched T waves. Drug-induced triangulation can be caused by blockade of I_{Kr}, but it can also be caused by blockade of other inward and outward currents. Triangulation results in a delayed and slower repolarization that means that a number of time-dependent elements in ion currents may be brought into play (Shah and Hondeghem, 2005). Among those that may lead to EAD, oscillations during repolarization, and possibly *torsades de pointes* are: longer time in the calcium and sodium current windows, longer time allowing reactivation of the calcium and sodium currents, and more time for depolarization by the sodium calcium exchange current (Hondeghem, 2007).

EAD can develop with prolonged APD and repetitive EADs may lead to triggered activity, which may perpetuate *torsades de pointes*. Moreover, EAD may also contribute to heterogeneity of AP configuration in the ventricle, and consequently to an increase in TDR. Therefore, EAD is also considered to play an important role in triggering *torsades de pointes* (Belardinelli et al., 2003).

2.2.3. Reverse frequency dependence

Many I_{Kr}-blockers prolong APD at low heart rate and the prolongation is less as heart rate is increased. This reverse frequency dependence is considered as a predictor of proarrhythmia (Shah and Hondeghem, 2005). During tachycardia the amplitude of I_{Ks} increases due to its slow deactivation while the amplitude of I_{Kr} remains nearly the same (Jurkiewicz and Sanguinetti, 1993). The contribution of I_{Kr} relative to I_{Ks} in AP repolarization is larger during bradycardia than during tachycardia. Therefore, I_{Kr}-blockers such as dofetilide and E4031 prolong APD more prominently during bradycardia (Martin et al., 1996; Matsuda et al., 2005; Toyama et al., 1997). However, I_{Kr}-blockers do not necessarily prolong APD in a reverse frequency-dependent manner. For example, amiodarone lacks reverse use dependence and torsadogenic risk. The positive inotropic agent vesnarinone inhibits HERG current in a voltage- and time-dependent manner (Katayama et al., 2000; Tsujimae et al., 2004), but, does not causes a reverse frequency-dependent prolongation of APD, while dofetilide and quinidine cause a reverse frequency-dependent prolongation of APD (Hatem et al., 1992; Toyama et al., 1997; Roden et al., 1987). Clinically, vesnarinone does not cause *torsades de pointes* but quinidine often does so (Feldman et al., 1991; Smith and Gallagher, 1980). Since both quinidine and vesnarinone inhibit HERG current in a voltage- and time-dependent manner (Katayama et al., 2000; Tsujimae et al., 2004), their different effects may be due to differences in their kinetics of HERG blockade where the development of block is much faster with quinidine than with vesnarinone (Katayama et al., 2000; Tsujimae et al., 2004). Therefore, the reverse frequency dependence of APD prolongation may reflect a specific aspect of I_{Kr}-blockade by drugs.

3. *In silico* risk assessment of drug-induced *torsades de pointes*

3.1. Problems with current risk assessment with electrophysiology

In the previous section, we presented an overview of current understanding of drug-induced cardiac arrhythmia, and in particular the electrophysiological indicators of the risk of *torsades de points*. But the accuracy of prediction of torsadogenic risk varies between different drugs and the outcome based on these predictive indicators is not satisfactory. There may be two major possible explanations for these discrepancies. The first explanation is that even if these drugs selectively inhibit I_{Kr}, they do so with distinct kinetics and thus the phenotype of alteration of the AP may differ. This can affect their torsadogenic potential (see Section 2.2.3). The other explanation is that some drugs may not be selective for I_{Kr} and that the cardiac arrhythmias could be generated not by a single mechanism but by multiple mechanisms.

Therefore, the further development of prediction methods for risk assessment is awaited to increase safety in drug usage in clinics and new drug development. An *in silico* strategy has particular merits for this purpose, because, different from purely experimental approaches, it can deal separately with the diverse actions of the drugs. For example, firstly, one can develop comprehensive and quantitative methods for assessing the risk caused by selective I_{Kr}-blockade and then, the method can be extended step by step to include the risks due to complex and/or non-specific actions of the drugs.

In this section, we will overview the current *in silico* methods for the assessment of the risks caused by selective I_{Kr}-blockade and their limitations, then we shall introduce a novel method for comprehensive assessment which we have developed recently. Future development of this method for more complex actions of drugs will also be discussed.

3.2. Currently available in silico *risk-assessment methods for selective* I_{Kr}*-blockade-induced cardiac arrhythmias*

In order to predict the risk of selective I_{Kr}-blockade inducing *torsades de pointes*, *in silico* approaches, including the prediction of an HERG channel blocking pharmacophore, have been used for a long time. However, pharmacophores determined from the ability of diverse structural compounds shown to block I_{Kr} cannot distinguish between those aspects of the compounds which cause I_{Kr} block, APD elongation and *torsades de pointes* from those that cause I_{Kr} block and APD elongation without any clinical association with *torsades de pointes*. Therefore, this method may overestimate the torsadogenic potential of chemical compounds. It is thus clear that more complex assays for the effects of I_{Kr} blocking drugs are required to more accurately evaluate any proarrhythmic risk.

On the other hand, *in silico* constructions of ventricular APs can provide some estimate of the mechanisms which could underlie proarrhythmic indicators such as AP triangulation and the production of EADs (e.g. Noble and Varghese, 1998; Viswanathan and Rudy, 1999; Noble and Noble, 2006). However, conventional approaches with AP models have problems with the new criteria of proarrhythmic risk mentioned above. For example, in the original formulation of I_{Kr} and I_{Ks} in the Luo–Rudy model (Faber and Rudy, 2000), I_{Kr}-blockade cannot substantially elongate APD at cycle lengths of 0.3, 1 or 3 s because the original large I_{Ks} conductance provides a too large repolarization reserve (Fig. 1, top). Only after the density of I_{Ks} is reduced to 40% of the original can I_{Kr}-blockade significantly elongate APD and induce EAD (Fig. 1, bottom). Therefore, with a single model with a single set of maximal conductance values, it is difficult to perform risk assessment for various I_{Kr}-blockers in a quantitative manner.

Also, worsening TDR is a substrate for cardiac arrhythmias independently of APD prolongation. To conduct analysis of TDR requires at least three different cardiac AP models representing endocardial, midcardial and epicardial myocytes in the ventricular wall. The role of TDR in cardiac arrhythmias may be related to differential reactions to I_{Kr}-blockade in the different types of myocytes.

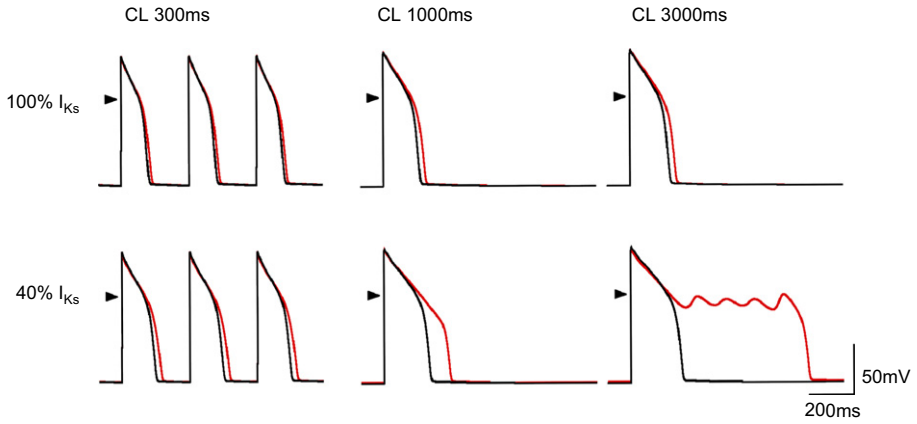

Fig. 1. Ventricular action potentials simulated with different conductance levels for I_{Kr} and I_{Ks}. Simulated action potentials at cycle lengths of 0.3, 1, 3 s with (top, black) $I_{Ks} = 100\%$ and $I_{Kr} = 100\%$, (top, red) $I_{Ks} = 100\%$ and $I_{Kr} = 20\%$, (bottom, black) $I_{Ks} = 40\%$ and $I_{Kr} = 100\%$ and (bottom, red) $I_{Ks} = 40\%$ and $I_{Kr} = 20\%$.

Also, considering that different I_{Kr}-blockers exhibit different blockade kinetics and proarrhythmic risk (see Section 2.2.3), a detailed knowledge of the kinetics of action of blockers of I_{Kr} is required in order to more adequately evaluate their effects on different types of ventricular myocyte and at different cycle lengths. Therefore, there is a clear need for developing a method that provides quantitative and comprehensive comparison of the effects of different forms of I_{Kr}-blockade upon APDs and TDR.

3.3. *Two-dimensional maps of action potential duration depending on* I_{Kr} *and* I_{Ks}

To assess the risk of drugs inducing life-threatening cardiac arrhythmias *in silico*, it is necessary to compare their effects on at least two points: (1) APDs in cardiac myocytes and (2) TDR in cardiac tissue. This review will introduce a novel method that can quantitatively and comprehensively evaluate cardiac electrical stability with drug-induced APD prolongation and TDR. This method is also able to explain the difference in the risk of different I_{Kr}-channel blockers. We propose a two-dimensional mapping method to interpret the effects of various drugs on APD and TDR in cardiac tissue (Suzuki et al., 2007). Computer models are used to calculate APD and TDR which are then plotted on a map whose axes are I_{Kr} and I_{Ks}. The different voltage- and time-dependent block of I_{Kr} is selected as being characteristic of different drug action. I_{Kr}-blockade can be classified into three representative groups: voltage- and time-independent blockade (e.g. dofetilide, E4031), fast voltage- and time-dependent blockade (e.g. quinidine), and slow

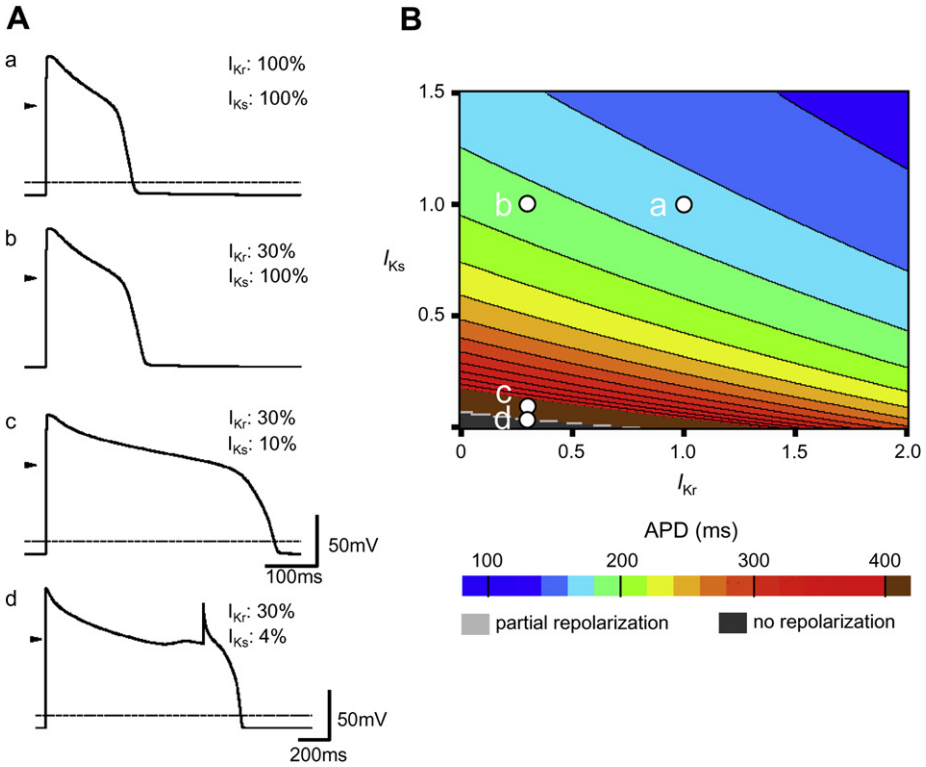

Fig. 2. The effects of varying the conductance of I_{Kr} and I_{Ks} upon APD. (A) Examples of action potentials simulated with different levels of I_{Kr} and I_{Ks} conductance (a) $I_{Kr} = 100\%$, $I_{Ks} = 100\%$; (b) $I_{Kr} = 30\%$, $I_{Ks} = 100\%$; (c) $I_{Kr} = 30\%$, $I_{Ks} = 10\%$; (d) $I_{Kr} = 30\%$, $I_{Ks} = 4\%$. Arrow heads indicate 0 mV membrane potential. (B) A two-dimensional map of APD simulated at a cycle length of 1 s. Vertical and horizontal axes represent the relative conductance of I_{Ks} and I_{Kr}, respectively, where a value of 1.0 represents those of the control model. Isolines linking equal APD were drawn at 20 ms intervals between 100 and 400 ms and the spaces between them were shaded from blue to red. APDs greater than 400 ms are shaded brown. Grey areas indicate regions where one or more AP simulations were longer than cycle length (Fig. 2A(d)).

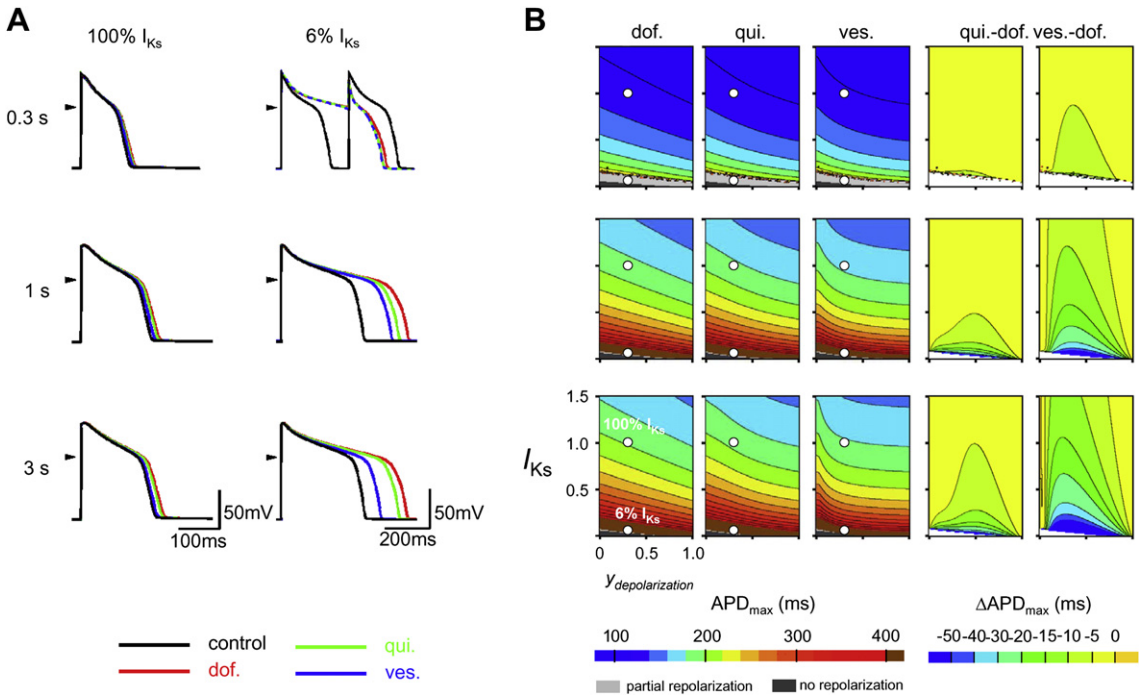

Fig. 3. A comparison of the effects of dofetilide, quinidine and vesnarinone blockade of I_{Kr} upon APD. (A) Simulated action potentials at cycle lengths of 0.3, 1, 3 s with $I_{Ks} = 100$ or 6% and $y_{depolarization} = 30\%$. (B) 2D maps of APD for each blockade type and maps of the difference between the effects of dofetilide and quinidine or vesnarinone. The horizontal axis represents the limit set for the minimum of unblocked I_{Kr} in the presence of drug i ($y_{depolarization,i}$). For dofetilide blockade, $y_{depolarization}$ and the fraction of I_{Kr} that is not blocked by drug i ($y(t)$) are the same at any time and voltage.

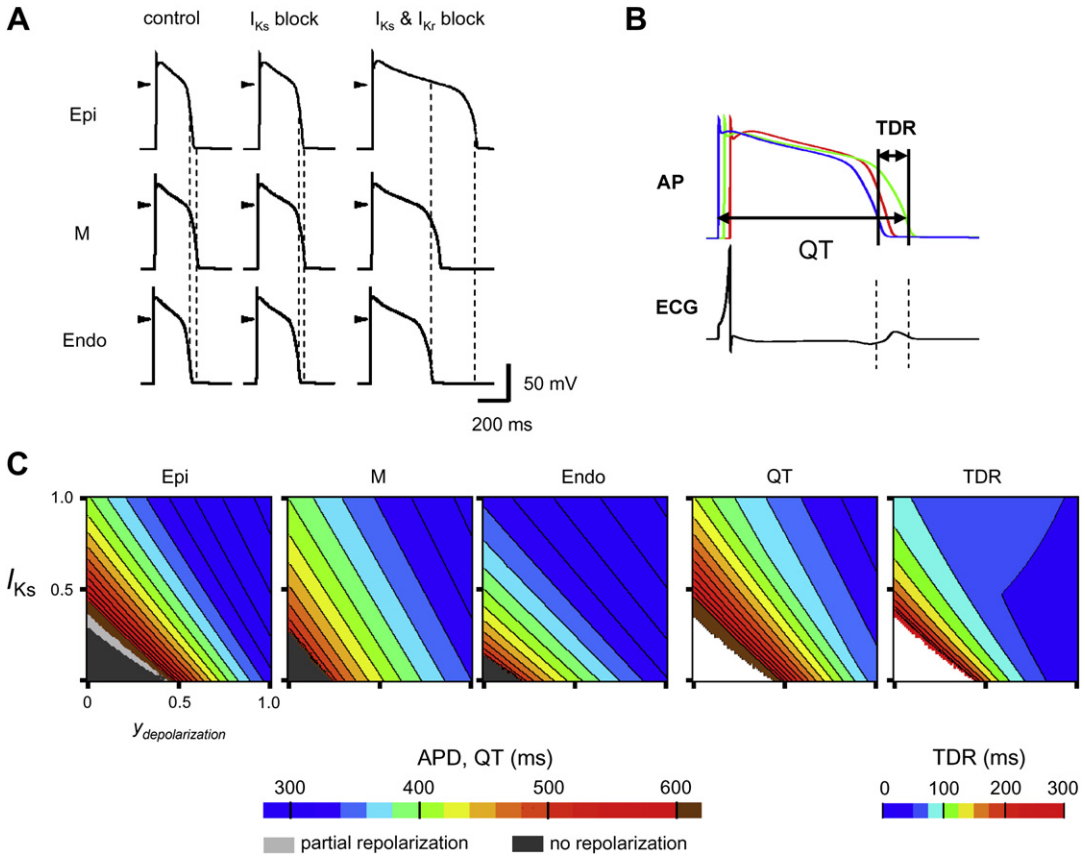

Fig. 4. Action potentials simulated in myocytes in the epicardial (Epi), midcardial (M), and endocardial (Endo) regions of the ventricle. (A) Simulated action potentials in the three types of myocyte and in the presence of I_{Kr} and/or I_{Ks} blockers at a cycle length of 2 s. The unblocked fraction of I_{Ks} was 29.74% and that of I_{Kr} was 7.431%. (B) Definition of the pseudo-QT and TDR. The pseudo-QT was defined as the interval between the first depolarization (blue) and the last repolarization in the myocardium (green), and the TDR was the interval between the first repolarization (blue) and the last repolarization in the myocardium (green). The pseudo ECG was calculated by summing the current flowing along 55 endo-, 55 M-, and 55 endo-myocytes, connected in a line. (C) 2D maps of APD in each type of myocyte and QT and TDR. White areas in QT and TDR maps indicate zones where at least one of the simulated APs was longer than the cycle length and it was not possible to calculate either QT or TDR.

voltage- and time-dependent blockade (e.g. vesnarinone). When the model is modified to reproduce APs in the epicardial, midcardial and endocardial myocardium, pseudo-electrocardiogram, QT interval and TDR can be simulated and the effects of drugs can be determined and the difference in the risk of a drug inducing life-threatening cardiac arrhythmias can be accounted for.

To develop 2D mapping of APD, we used a modified version of the Luo and Rudy phase II (LRd) ventricular myocyte model (Luo and Rudy, 1994; Zeng et al., 1995; Viswanathan et al., 1999; Faber and Rudy, 2000) where the L-type Ca^{2+} channel formulation was replaced by a model that can differentiate the VDI and CDI mechanisms (Findlay et al., 2008 and see Appendix 1). Equilibrium was achieved by running the model for 30 cycles. ADP was measured at −75 mV (close to APD_{90}) and the longest APD value recorded from the final 10 APs was used for the construction of the map. The 2D map was constructed by repeating the cycle of 30 AP simulations and systematically varying the maximum possible conductance of I_{Ks} in increments of 1% and systematically varying I_{Kr} according to the type of blockade. We adopted the relatively small number of APs (30) because of common intrinsic problems with a steady state in many ventricular models, including the LRd model and its many variants such as ours in this study. For example, steady-state intracellular Na^+ concentration is very high and this strongly affects Na^+ dependent currents (e.g. I_{NaK} and I_{NaCa}) and consequently steady-state APD, which is not very likely in normal physiological conditions. Therefore, we decided to use a compromise between the initial and the steady-state, i.e. 30 cycles, where intracellular Na^+ concentration is not too high and tuning the AP by varying K^+ channel currents could reproduce the experiments of Aiba et al. (2005). This compromise did not affect the purpose and conclusion in this study which shows how to pull out the systematic features of the AP under application of I_{Kr}-blockers and use them for the assessment of the risk of drug-induced cardiac arrhythmias.

Fig. 2 illustrates individual simulated APs and the basic 2D map of APD resulting from varying the relative conductance of I_{Kr} (horizontal axis) and I_{Ks} (vertical axis) with a cycle length of 1 s. The two-dimensional display clearly shows that alterations of I_{Kr} and I_{Ks} have different degrees of effect on APD. The steeper the slope of an isoline, the larger is the relative contribution of I_{Kr} to APD. The shallower the slope of an isoline, the larger is the relative contribution of I_{Ks} to APD. The space between the isolines reflects the degree of stability of APD. In areas where isolines are widely spaced, APD is relatively insensitive to alterations in the conductance of I_{Kr} and/or I_{Ks}. On the other hand, when isolines are close together, APD can be altered by even slight modulation of I_{Kr} and/or I_{Ks}. Thus, in this method, the systematic property of APD depending on repolarization reserve (i.e. I_{Kr} and I_{Ks}) can be evaluated quantitatively and comprehensively.

3.4. 2D map analysis of the different types of I_{Kr}-blockade on the ventricular APD

We examined the usefulness of this method to evaluate the difference between various types of I_{Kr}-blockade (Fig. 3). We constructed models (Appendix 2) of three representative types of blockade typified by dofetilide, quinidine and vesnarinone. Fig. 3A illustrates the effects of the three types of blockade of I_{Kr} on APs at different cycle length. When the model used the original I_{Kr} and I_{Ks} conductance values (Faber and Rudy, 2000), none of the agents substantially prolonged APD at any cycle length (Fig. 3A, 100% I_{Ks}). The absence of an effect of I_{Kr}-blockade was due to the original large I_{Ks} conductance which provided a repolarization reserve in the model that compensated for strong inhibition of I_{Kr}. When the maximum value for the I_{Ks} conductance was reduced to 6% of the original, this effect was lost and each of the agents affected APD. Dofetilide and quinidine blockade prolonged APD more than vesnarinone. It is therefore clear that in order to properly evaluate the proarrhythmic effect of an "HERG-channel-blocker", it is necessary to measure not only its effect upon I_{Kr} but also the influence of variation of I_{Ks}. The 2D map incorporates variation of I_{Ks}, with both inhibition (relative conductance < 1) and excitation (relative conductance > 1).

Fig. 3B illustrates 2D maps of APD showing the effects of the three types of I_{Kr}-blockade at three different cycle lengths (0.3, 1 and 3 s). In dofetilide blockade the red areas corresponding to long APD increased with increasing cycle length and the slopes of the isolines became steeper. This indicates that the relative contribution of I_{Kr} over I_{Ks} for AP repolarization increases with an increase in cycle length. This change of isoline slope is an expression of reverse frequency-dependent prolongation of APD by a drug. The reverse frequency dependence of APD prolongation is a critical indicator of drug-induced cardiac arrhythmia which simple simulations of an AP would miss in the presence of a large repolarization reserve due to abundant I_{Ks}. The 2D map analysis of I_{Kr}–I_{Ks} eliminates this defect.

The voltage- and time-dependent blockade of I_{Kr} by quinidine induced curvature of the isolines which was even more prominent

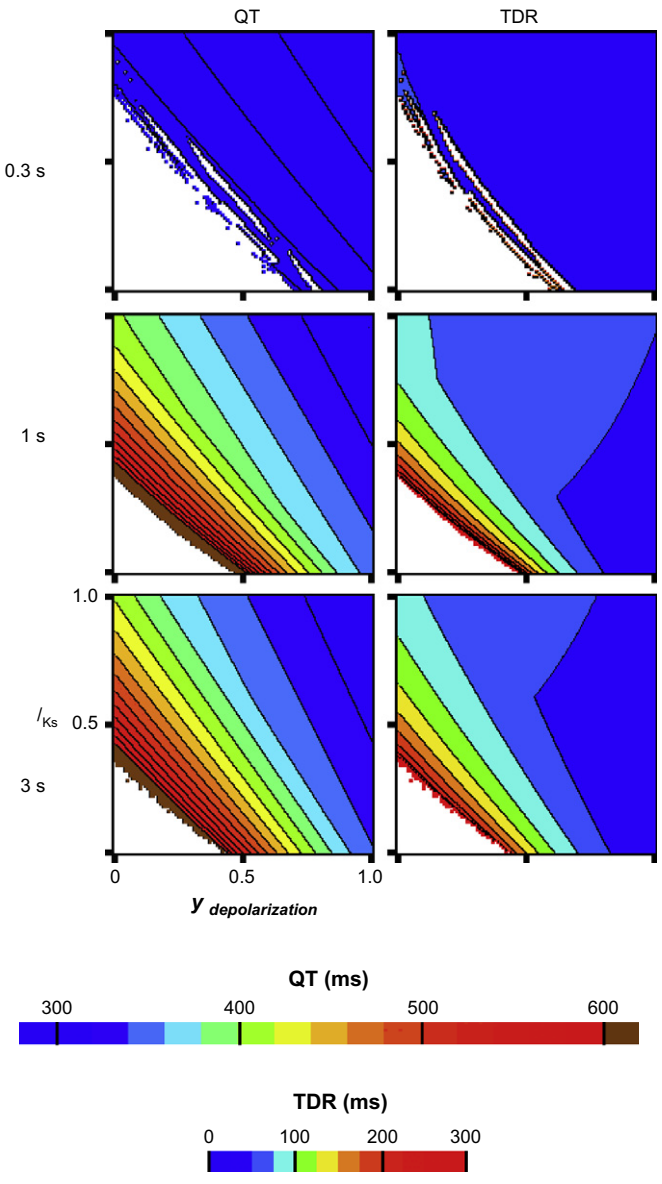

Fig. 5. The effects of cycle length upon 2D maps of QT and TDR.

under vesnarinone blockade. This was particularly evident at a cycle length of 3 s. This means that the blockade of I_{Kr} by vesnarinone may not cause significant prolongation of APD until $y_{depolarization}$ is reduced to ~0.2 and since the isolines were almost horizontal over a considerable range of inhibition of I_{Kr} (from 1 to 0.3 of $y_{depolarization}$) APD prolongation depended mainly on I_{Ks} and not on I_{Kr}. Therefore, it is expected that vesnarinone-type I_{Kr}-blockers would show little effect on APD in this range.

This characteristic of the time- and voltage-dependent drugs was further analyzed by subtracting the effect of voltage- and time-independent block (Fig. 3B, right). Negative values indicate where these drugs had less of an effect upon APD than dofetilide. It was noticeable that vesnarinone blockade was weaker at longer cycle length and since less APD prolongation at slow stimulus frequency is a preferable character for a drug, this analysis suggests that a vesnarinone-type of blocker may be safer than the other drugs. Indeed, vesnarinone is not associated with ventricular arrhythmias (Feldman et al., 1991) while dofetilide and quinidine often cause *torsades de pointes* (Smith and Gallagher, 1980; Torp-Pedersen et al., 2000).

These results indicate the utility of 2D mapping with a single standardized ventricular myocyte. But, the idea can also be extended to a more physiologically relevant model involving the variation of AP types and the transmission of APs across the ventricular wall.

3.5. Transmural ventricular AP models

Based on the general ventricular myocyte model, we developed three models representative of cardiomyocytes in the epicardium (Epi), mesocardium (M), and endocardium (Endo) of the ventricle. Fig. 4A shows simulated APs for cardiomyocytes in the Epi, M, and Endo regions in control conditions, in the presence of I_{Ks} block, and in the presence of both I_{Kr} and I_{Ks} block. These models were derived by adjusting the parameters of the maximum conductances of K^+ channel currents (I_{Kr}, I_{Ks}, I_{to}, I_{Kp}) to reproduce the experimental data of Aiba et al. (2005) (Table 1) so that in control and in the presence of I_{Ks} block, APDs of M cells are slightly longer than those of the other myocyte types; and in the presence of I_{Kr} and I_{Ks} block the APD in Epi is the most prolonged.

The 2D maps of APD dependent upon variation in I_{Ks} and I_{Kr} for each layer of the myocardium are shown in Fig. 4C. The different orientations of the isolines in these maps reveal a divergent dependence of APD on I_{Kr} and I_{Ks} in each layer. Pseudo-QT and TDR values were obtained for each combination of I_{Kr} and I_{Ks} (Fig. 4C). Since these three models were not assembled to represent a 3D cross-section of the ventricle wall, to construct the QT and TDR maps the timing of the excitation of each type of myocyte corresponded to their approximate position and transmural conduction (Aiba et al., 2005). Thus the endocardium model was stimulated first, the M cell after 9 ms and the epicardium after a further 9 ms. The QT interval was easily prolonged by the reduction of either I_{Kr} and/or I_{Ks} while a serious elongation of TDR required both I_{Kr} and I_{Ks} to be reduced to less than approximately half of the control values. The very narrow area of the 2D map over which TDR then elongated (yellow to red scale in Fig. 4C) may represent a critical zone of proarrhythmic risk.

Fig. 5 shows 2D maps of QT interval and TDR at three different cycle lengths. At a cycle length of 0.3 s, simulations of APD with reduced I_{Kr} and/or I_{Ks} easily overran the cycle length (white areas). At cycle lengths of 1 and 3 s there were no marked differences between the 2D maps for either QT interval or TDR. There was a slight tendency for an expansion of the distance between isolines at a cycle length of 3 s. This analysis clearly indicates that the effects of changing cycle length upon QT interval and TDR (Fig. 5) are different from those upon APD in a standardized ventricular myocyte (Fig. 3).

3.6. Two dimension map analysis of the effects of different types of I_{Kr}-blockade on ventricular transmural dispersion of repolarization

Fig. 6A displays 2D maps of QT interval and TDR obtained under blockade of I_{Kr} by dofetilide, quinidine, and vesnarinone. The drugs showing time- and voltage-dependent block of I_{Kr} induced less QT prolongation, in particular vesnarinone. The TDR map shows alterations in the proarrhythmic risk for each drug more clearly. The area at risk (yellow to red scale) is reduced and shifted to the left by vesnarinone. The reduction of TDR related to time- and voltage-dependent blockade of I_{Kr} at different cycle lengths is shown in Fig. 6B. Vesnarinone induced

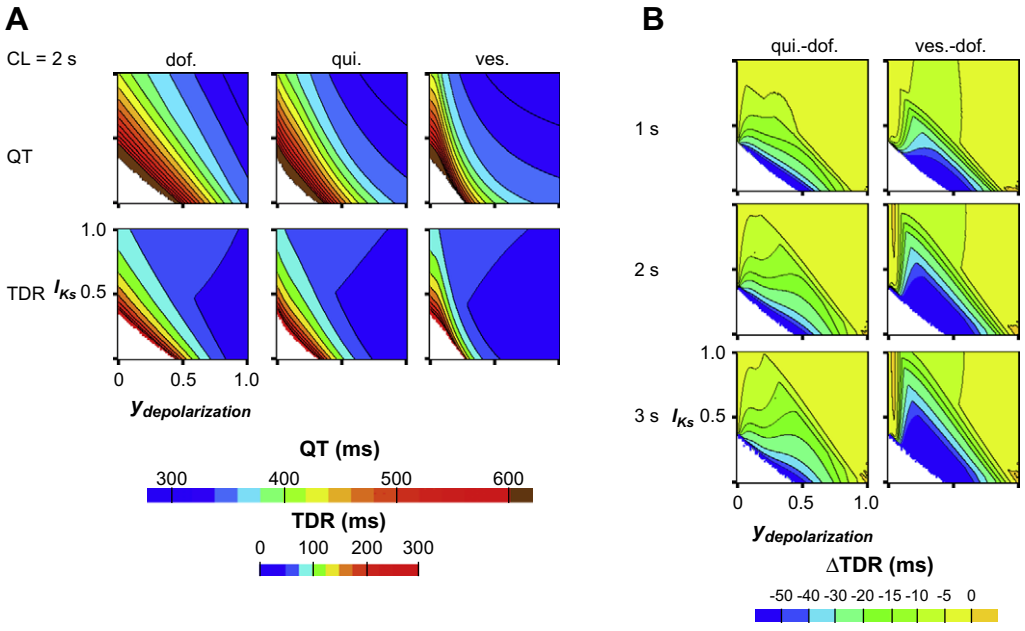

Fig. 6. The effects of dofetilide, quinidine and vesnarinone on QT and TDR. (A) 2D maps of QT and TDR in the presence of each drug type (cycle length 2 s). (B) 2D maps of differences between TDR (quinidine) – TDR (dofetilide) and TDR (vesnarinone) – TDR (dofetilide) at cycle lengths of 1, 2 and 3 s, respectively.

less TDR dispersion than quinidine at each cycle length. Increasing cycle length reduced TDR dispersion in particular under vesnarinone. Therefore, according to these simulations, the strength of the drugs' reverse frequency-dependent effects on TDR are dofetilide > quinidine > vesnarinone.

4. Limitations and further directions for 2D map expression

One of the advantages of the 2D mapping method is that this technique can be applied to any cardiac cell model. For example, this approach could be useful to analyze the effects of channel modulation on atrial excitability. In human atrial myocytes the short APD is due more to I_{Kur} and I_{to} than I_{Kr} and I_{Ks} (Courtemanche et al., 1999). In which case, I_{Kur} and I_{to} could form the axes of 2D maps. The database of CellML models (http://www.cellml.org/) is a great resource for testing this method upon a variety of cardiac myocyte models.

With this 2D map method, the influence of other ion channels on APD can also be examined systematically. This type of analysis should also be useful to assess the proarrhythmic or antiarrhythmic effects of modulation of multiple ion channels and therefore aid to evaluate treatment strategies for drug-induction of cardiac arrhythmias. In preliminary tests, 2D maps of I_{Ks}/I_{Kr} showed that TDR due to an I_{Kr} blocker was decreased in the presence of a Ca^{2+} channel blocker and increased in the presence of a Na^{+} channel blocker (not shown). This suggests that these types of analysis may be useful to analyze interactions between drugs' effects.

The major limitation of this method at present is that the effect of conduction through the heart wall has not been included in the calculation of TDR. The simple method to calculate TDR used here is clearly not enough and should be improved. This will require the development of a 3D ventricular wall model which is composed of endocardial, midcardial and epicardial layers with conduction of APs across the wall.

The 2D map analysis method and its application to a proper model for the conducting ventricular wall model will provide valuable information concerning the relationship between APD, ion channel density, and the characteristics of the effects of ion channel blockers on APD, and TDR.

Appendix. Supplementary data

Supplementary data associated with this article can be found, in the online version, at doi:10.1016/j.pbiomolbio.2008.05.003.

References

Aiba, T., Shimizu, W., Inagaki, M., Noda, T., Miyoshi, S., Ding, W.G., Zankov, D.P., Toyoda, F., Matsuura, H., Horie, M., Sunagawa, K., 2005. Cellular and ionic mechanism for drug-induced long QT syndrome and effectiveness of verapamil. J. Am. Coll. Cardiol. 45, 300–307.

Belardinelli, L., Antzelevitch, C., Vos, M.A., 2003. Assessing predictors of drug-induced torsade de pointes. Trends Pharmacol. Sci. 24, 619–625.

Courtemanche, M., Ramirez, R.J., Nattel, S., 1999. Ionic targets for drug therapy and atrial fibrillation-induced electrical remodeling: insights from a mathematical model. Cardiovasc. Res. 42, 477–489.

Faber, G.M., Rudy, Y., 2000. Action potential and contractility changes in $[Na^{+}]_i$ overloaded cardiac myocytes: a simulation study. Biophys. J. 78, 2392–2404.

Feldman, A.M., Baughman, K.L., Lee, W.K., Gottlieb, S.H., Weiss, J.L., Becker, L.C., Strobeck, J.E., 1991. Usefulness of OPC-8212, a quinolinone derivative, for chronic congestive heart failure in patients with ischemic heart disease or idiopathic dilated cardiomyopathy. Am. J. Cardiol. 68, 1203–1210.

Findlay, I., Suzuki, S., Murakami, S., Kurachi, Y., 2008. Physiological modulation of voltage-dependent inactivation in the cardiac muscle L-type calcium channel: a modelling study. Prog. Biophys. Mol. Biol. 96, 482–498.

Hatem, S., Le Grand, B., Le Heuzey, J.Y., Couetil, J.P., Deroubaix, E., 1992. Differential effects of quinidine and flecainide on plateau duration of human atrial action potential. Basic Res. Cardiol. 87, 600–609.

Hoffmann, P., Warner, B., 2006. Are hERG channel inhibition and QT interval prolongation all there is in drug-induced torsadogenesis? A review of emerging trends. J. Pharmacol. Toxicol. Methods 53, 87–105.

Hondeghem, L.M., 2000. Frequency dependence of class I and class III antiarrhythmic agents explaining their antiarrhythmic and proarrhythmic properties. In: Franz, M.R. (Ed.), Monophasic Action Potentials. Futura Publishing, Mount Kisco, NY, pp. 381–394.

Hondeghem, L.M., 2006. Thorough QT/QTc not so thorough: removes torsadogenic predictors from the T-wave, incriminates safe drugs, and misses profibrillatory drugs. J. Cardiovasc. Electrophysiol. 17, 337–340.

Hondeghem, L.M., 2007. Relative contributions of TRIaD and QT to proarrhythmia. J. Cardiovasc. Electrophysiol. 18, 655–657.

Hondeghem, L.M., Hoffmann, P., 2003. Blinded test in isolated female rabbit heart reliably identifies action potential duration prolongation and proarrhythmic drugs: importance of triangulation, reverse use dependence, and instability. J. Cardiovasc. Pharmacol. 41, 14–24.

Jurkiewicz, N.K., Sanguinetti, M.C., 1993. Rate-dependent prolongation of cardiac action potentials by a methanesulfonanilide class III antiarrhythmic agent. Specific block of rapidly activating delayed rectifier K^{+} current by dofetilide. Circ. Res. 72, 75–83.

Kannankeril, P.J., Roden, D.M., 2007. Drug-induced long QT and torsade de pointes: recent advances. Curr. Opin. Cardiol. 22, 239–243.

Katayama, Y., Fujita, A., Ohe, T., Findlay, I., Kurachi, Y., 2000. Inhibitory effects of vesnarinone on cloned cardiac delayed rectifier K^{+} channels expressed in a mammalian cell line. J. Pharmacol. Exp. Ther. 294, 339–346.

Kuryshev, Y.A., Brown, A.M., Wang, L., Benedict, C.R., Rampe, D., 2000. Interactions of the 5-hydroxytryptamine 3 antagonist class of antiemetic drugs with human cardiac ion channels. J. Pharmacol. Exp. Ther. 295, 614–620.

Lawrence, C.L., Pollard, C.E., Hammond, T.G., Valentin, J.P., 2005. Nonclinical proarrhythmia models: predicting torsades de pointes. J. Pharmacol. Toxicol. Methods 52, 46–59.

Liu, X.K., Katchman, A., Ebert, S.N., Woosley, R.L., 1998. The antiestrogen tamoxifen blocks the delayed rectifier potassium current, IKr, in rabbit ventricular myocytes. J. Pharmacol. Exp. Ther. 287, 877–883.

Luo, C.H., Rudy, Y., 1994. A dynamic model of the cardiac ventricular action potential. I. Simulations of ionic currents and concentration changes. Circ. Res. 74, 1071–1096.

Martin, C.L., Palomo, M.A., Mcmahon, E.G., 1996. Comparison of bidisomide, flecainide and dofetilide on action potential duration in isolated canine atria: effect of isoproterenol. J. Pharmacol. Exp. Ther. 278, 154–162.

Matsuda, T., Takeda, K., Ito, M., Yamagishi, R., Tamura, M., Nakamura, H., Tsuruoka, N., Saito, T., Masumiya, H., Suzuki, T., Iida-Tanaka, N., Itokawa-Matsuda, M., Yamashita, T., Tsuruzoe, N., Tanaka, H., Shigenobu, K., 2005. Atria selective prolongation by NIP-142, an antiarrhythmic agent, of refractory period and action potential duration in guinea pig myocardium. J. Pharmacol. Sci. 98, 33–40.

Morganroth, J., 1993. Relations of QTc prolongation on the electrocardiogram to torsades de pointes: definitions and mechanisms. Am. J. Cardiol. 72, 10B–13B.

Noble, D., Noble, P.J., 2006. Late sodium current in the pathophysiology of cardiovascular disease: consequences of sodium–calcium overload. Heart 92, iv1–iv5.

Noble, D., Varghese, A., 1998. Modeling of sodium–calcium overload arrhythmias and their suppression. Can. J. Cardiol. 14, 97–100.

Roden, D.M., 2004. Drug-induced prolongation of the QT interval. N. Engl. J. Med. 350, 1013–1022.

Roden, D.M., Iansmith, D.H., Woosley, R.L., 1987. Frequency-dependent interactions of mexiletine and quinidine on depolarization and repolarization in canine Purkinje fibers. J. Pharmacol. Exp. Ther. 243, 1218–1224.

Sanguinetti, M.C., Jurkiewicz, N.K., 1990. Two components of cardiac delayed rectifier K^{+} current. Differential sensitivity to block by class III antiarrhythmic agents. J. Gen. Physiol. 96, 195–215.

Sanguinetti, M.C., Jurkiewicz, N.K., 1991. Delayed rectifier outward K^{+} current is composed of two currents in guinea pig atrial cells. Am. J. Physiol. 260, H393–H399.

Shah, R.R., Hondeghem, L.M., 2005. Refining detection of drug-induced proarrhythmia: QT interval and TRIaD. Heart Rhythm 2, 758–772.

Smith, W.M., Gallagher, J.J., 1980. "Les torsades de pointes": an unusual ventricular arrhythmia. Ann. Intern. Med. 93, 578–584.

Suzuki, S., Tsujimae, K., Murakami, S., Findlay, I., Kurachi, Y., 2007. Two-dimensional mapping of cardiac action potential duration for assessing the risk of drug-induced arrhythmia. The Proceedings of the 80th Annual Meeting of the Japanese Pharmacological Society, March 14–16, 2007, Nagoya, Japan. Abst. J. Pharmacol. Sci. 103 (Suppl. I), 196.

Taylor, D., 2003. Ziprasidone in the management of schizophrenia. CNS Drugs 17, 423–430.

Torp-Pedersen, C., Brendorp, B., Kober, L., 2000. Dofetilide: a class III anti-arrhythmic drug for the treatment of atrial fibrillation. Expert. Opin. Investig. Drugs 9, 2695–2704.

Toyama, J., Kamiya, K., Cheng, J., Lee, J.K., Suzuki, R., Kodama, I., 1997. Vesnarinone prolongs action potential duration without reverse frequency dependence in rabbit ventricular muscle by blocking the delayed rectifier K^{+} current. Circulation 96, 3696–3703.

Tsujimae, K., Suzuki, S., Yamada, M., Kurachi, Y., 2004. Comparison of kinetic properties of quinidine and dofetilide block of HERG channels. Eur. J. Pharmacol. 493, 29–40.

Van Opstal, J.M., Schoenmakers, M., Verduyn, S.C., de Groot, S.H., Leunissen, J.D., van Der Hulst, F.F., Molenschot, M.M., Wellens, H.J., Vos, M.A., 2001. Chronic amiodarone evokes no torsade de pointes arrhythmias despite QT lengthening in an animal model of acquired long-QT syndrome. Circulation 104, 2722–2727.

Viswanathan, P.C., Rudy, Y., 1999. Pause induced early afterdepolarizations in the long QT syndrome: a simulation study. Cardiovasc. Res. 42, 530–542.

Viswanathan, P.C., Shaw, R.M., Rudy, Y., 1999. Effects of I_{Kr} and I_{Ks} heterogeneity on action potential duration and its rate dependence: a simulation study. Circulation 99, 2466–2474.

Wang, S., Liu, S., Morales, M.J., Strauss, H.C., Rasmusson, R.L., 1997. A quantitative analysis of the activation and inactivation kinetics of HERG expressed in *Xenopus oocytes*. J. Physiol. 502, 45–60.

Warner, B., Hoffmann, P., 2002. Investigation of the potential of clozapine to cause torsade de pointes. Adverse Drug React. Toxicol. Rev. 21, 189–203.

Yan, G.X., Antzelevitch, C., 1998. Cellular basis for the normal T wave and the electrocardiographic manifestations of the long-QT syndrome. Circulation 98, 1928–1936.

Zeng, J., Kenneth, R., Laurita, K.R., Rosenbaum, D.S., Rudy, Y., 1995. Two components of the delayed rectifier K^+ current in ventricular myocytes of the guinea-pig type. Theoretical formulation and their role in repolarization. Circ. Res. 77, 140–152.